Diamond & Related Materials 80 (2017) 147–152

Contents lists available at ScienceDirect

Diamond & Related Materials

journal homepage: www.elsevier.com/locate/diamond

Direct observation of electron emission from CVD diamond grain boundaries by tunnelling atomic force microscopy independent of surface morphology

Robert Harniman[a], Paul W. May[a,*], Oliver J.L. Fox[a,b]

[a] School of Chemistry, University of Bristol, Cantock's Close, Bristol BS8 1TS, United Kingdom
[b] Diamond Light Source Ltd., Harwell Science and Innovation Campus, Didcot, Oxfordshire OX11 0DE, United Kingdom

A B S T R A C T

We present direct observation of the electron field emission sites over a large area of polycrystalline diamond using tunnelling atomic force microscopy. Any effects of surface topography have been reduced by measuring polycrystalline samples which have surface roughness values < 5 nm. Measurements show that emission arises preferentially from the grain boundaries independent of the surrounding surface morphology.

1. Introduction

Chemical vapour deposition (CVD) of diamond has now become a mature technology, which is being used to fabricate diamond thin films for an increasing number of applications [1]. The hydrogen termination present on the surface of most CVD diamond films imparts negative electron affinity (NEA), which lowers the effective surface potential barrier that electrons must overcome to escape into vacuum [2]. This NEA surface makes CVD diamond a candidate for a range of electron emission devices, including electron sources/guns (for microwave tubes or high-definition television), radio-frequency electron injectors [3], cathodes for photoinjectors [4], thermionic heat convertors (for solar power generation and heat-scavenging devices) [5], and high-gain secondary electron emission emitters (for photomultiplier tubes and amplified night-vision goggles) [6]. Extraction of electrons from a diamond surface via application of a large applied electric field (field emission) has been studied as a possible route for bright, emissive display technology [7] or fast-switching vacuum electronics [8]. Unlike field emission from metals, which has been understood for nearly 90 years [9], the mechanism for field emission from a wide band-gap semiconductor, such as low-conductivity polycrystalline CVD diamond, remains poorly understood.

Field emission from diamond films is usually measured in a high-vacuum chamber, where the diamond film is attached to a grounded holder while a positively biased electrode is positioned 10–100 μm above the film surface. As the voltage bias on the electrode is increased, above some threshold voltage, V_{th}, electrons begin to be extracted from the diamond surface, travel across the vacuum gap and are collected by the electrode. Above V_{th}, the measured emission current is a function of the bias voltage and follows the Fowler-Nordheim model for field emission, which was originally devised for electron emission from metals by quantum mechanical tunnelling through a potential barrier [9].

However, for a number of reasons, field emission from polycrystalline diamond (PCD) films is not as straightforward as that from many other materials. First, the polycrystalline nature of the film means that the surface contains both diamond crystallites surrounded by their corresponding grain boundaries (GBs). The crystallites are almost pure sp^3 diamond, while the GBs can be composed of sp^2 carbon, graphitic impurities, impurity atoms (such as H, B, etc.), stacking faults, etc., and can range in thickness from atomically sharp to several nm depending on the type of diamond film under test.

Second, faceted microcrystalline diamond (MCD) films grow via a van der Drift process which produces columnar growth structures [1]. This leads to a GB network that electrically connects the bottom of the film to its surface. In poorly conducting (undoped) diamond films, these vertical GBs act as conducting pathways for electrons to travel from the grounded substrate holder, through the film, to its surface, to be emitted at some specific location.

Another complication is that the measured emission current often originates from multiple emission sites [10], depending upon the area of the electrode used. Also, faceted PCD films exhibit wide variations in topography, with height differences from the top of peaks to the bottom of valleys varying from nm to 100 s of μm depending on the film. MCD facets can also exhibit sharp edges or apices which may increase field emission by enhancing the local electric field, while nanocrystalline diamond (NCD) often exhibits more rounded crystallite structures. In contrast, ultrananocrystalline diamond (UNCD) films can appear smooth on a nm scale, yet still field emit with high current at low bias values.

* Corresponding author.
E-mail address: paul.may@bristol.ac.uk (P.W. May).

http://dx.doi.org/10.1016/j.diamond.2017.09.009
Received 21 July 2017; Received in revised form 12 September 2017; Accepted 12 September 2017
Available online 20 September 2017

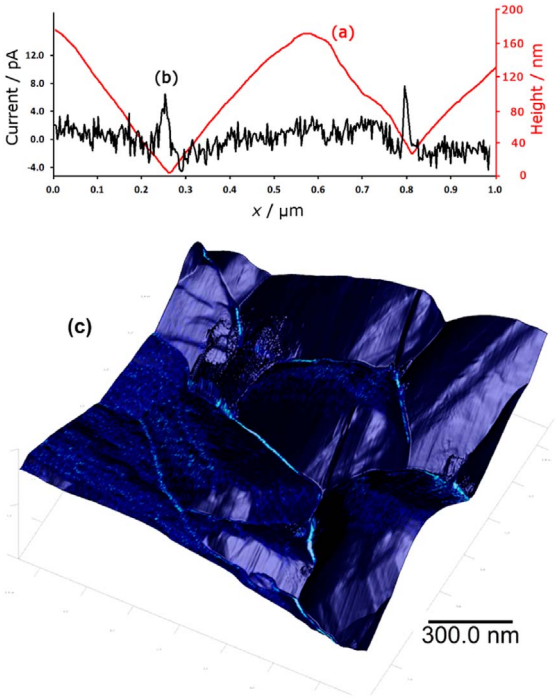

Fig. 1. PF-TUNA measurement (bias 3 mV) of topography and tunnelling current across a representative region of a freestanding MCD film. (a) A line profile of topography across a 0.5 µm facetted crystallite and 2 GBs. (b) The corresponding line profile for measured tunnelling current showing spikes in emission at the position of the GBs and not at the top of the peak. (c) 3D surface showing the topography with the corresponding emission current overlaid as a blue colour-map (the lighter the colour, the higher the emission current). (For interpretation of the references to colour in this figure legend, the reader is referred to the web version of this article.)

Further, CVD diamond films are usually terminated with hydrogen, and this imparts an NEA to the surface. This NEA surface is essential for efficient field emission at low bias, as it is believed to lower the barrier for electron emission. Exposing the H-terminated film to oxygen (or even leaving the sample in ambient air for a few days) is sufficient to replace some of the surface H with O groups, which degrades the NEA, reduces the percentage of the surface area emitting, and worsens the field emission performance [11]. In addition, there are many reports that state that in order to achieve stable and reproducible field emission, the bias must be cycled up and down a few times to 'condition' the surface. This conditioning process is believed to be a combination of many processes, including removing the H termination or other adsorbates, graphitisation of the surface and/or the conducting GB pathways, or even burning or restructuring of the surface morphology [12]. Finally, doping diamond with boron changes its electrical conductivity, which can be varied from highly insulating to near-metallic depending on the B content. Having a conducting PCD film changes the field emission characteristics yet again, as the electrons can now travel more easily through the film (via the GBs as before but now via the grains as well) to reach the surface.

All these issues have made field emission from diamond a tricky problem to study, and the mechanism by which it occurs has proven controversial. Considerable effort [8] has been spent on trying to process diamond into needles, cones, pyramids or other sharp-tipped structures, in the belief that the electric field enhancement around these structures is necessary for efficient electron emission. However, the experimentally measured field emission efficiency from such structures is significantly smaller than theory predicts, causing scientists to search for other mechanisms to explain the efficient emission from PCD films [13]. Many experiments show that field emission seems to correlate with the number and density of grain boundaries containing non-diamond sp^2 carbon [14]. In fact, single-crystal diamond shows little, if any, field emission. To explain this, Cui et al. [15] devised a mechanism in which the threshold for field emission is lowered due to a local reduction of the electron affinity of the diamond surface that surrounds nanosized graphitic surface structures, such as defects or grain boundaries. Field emission takes place from the graphitic region, but the emission barrier is controlled by the surrounding diamond. A similar model for the enhanced field emission from other forms of carbon, including flat, smooth, diamond-like carbon, was suggested by Robertson [16] and by Ilie et al. [17].

Despite a number of experimental reports providing circumstantial evidence in support of Cui et al.'s model, direct confirmation of GB emission has proven elusive. Recently, we demonstrated that electron emission in low conductivity polycrystalline diamond films originates from the grain boundaries (GBs) and not from sharp peaks, edges or other topographical features [11,18]. This observation provided compelling evidence for Cui et al.'s model for electron field emission [15], and confirmed the initial findings of previous groups [19,20,21]. Direct observation of the electron emission sites was achieved utilising PeakForce-controlled tunnelling atomic force microscopy (PF-TUNA[1]) in a low-force regime. In this system, a tunnelling current is measured between a sharp, conductive atomic force microscopy (AFM) tip and a sample surface as the tip tracks the sample topography. The advantages of PF-TUNA for the study of field emission on CVD diamond have been discussed previously, as well as the numerous precautions necessary to ensure that the recorded data correspond to reality and not to experimental artefacts [11]. Chubenko et al. [22] recently showed theoretically that, although the electron emission processes occurring during PF-TUNA measurements are not directly equivalent to those occurring during macro-scale field emission, tunnelling measurements can nevertheless be used to better understand and interpret data about field emission mechanisms and site locations.

For poorly conducting diamond films with granular morphology on the micron scale, the specific advantage of PeakForce control is that the interaction force between the tip and the sample is kept constant at a set-point value through the non-resonant collection of force curves while scanning, and therefore the tip-surface separation and the emission regime are also constant. This means that samples with a surface

[1] PeakForce and TUNA are trademarks of Bruker, the company that manufactures the PF-TUNA AFM system.

r.m.s. roughness of several microns can be investigated over scan areas up to hundreds of square microns, allowing a wider picture of the overall morphology to be obtained. Scans can then be performed over regions of a few microns with resolution in the range of nanometres, and with very high current sensitivity, which is particularly useful for the electrical characterisation of low-conductivity samples at high lateral resolution.

Detailed PF-TUNA investigation of CVD diamond films has shown that electron emission from GBs remains the dominant mechanism across a range of grain sizes [11] and topographies, including CVD diamond coated onto vertically aligned carbon nanotube 'teepee' structures [23]. An example of such data is shown in Fig. 1 for a free-standing undoped 10 μm-thick MCD film deposited using a hot filament diamond CVD reactor (20 Torr pressure, 1%CH_4/H_2, substrate temperature 900 °C, Ta filaments 2100 °C). The topography scan (Fig. 1(a)) shows that the crystallites are ~0.5 μm in size, while the corresponding line profile for the measured tunnelling current (Fig. 1(b)) shows peaks in emission matching the position of the GBs and not from the highest regions of the structures. This is highlighted further in the overlaid image in Fig. 1(c) where the lowest regions between the crystallites appear brighter than the crystallites themselves. In contrast, for doped PCD films with higher conductivity, electron emission is found to occur from the surface of the grains themselves, as well as the GBs [11]. With increasing conductivity, the effect of the lowering of the localised barrier by the presence of the GB is lessened with respect to emission from the crystallite surface elsewhere. As such, with increasing conductivity, electron emission starts to occur further up the grain until when the film is highly conducting, emission occurs uniformly from the grains and GBs alike.

We now extend the PF-TUNA investigation of the electron emission mechanism to the other end of the topographic scale - to 'smooth', low conductivity PCD films with surface features smaller than that of nanocrystalline diamond. Such smooth, flat films, effectively eliminate the influence of topography on PF-TUNA measurements, providing additional evidence that emission measured at GBs is not the result of AFM tip geometry interacting with surface features or other topographical structures. Chubenko et al. [22] state that the PF-TUNA mechanism has the potential to enable measurement of surface barrier structure, Fermi level positioning and the electron supply function of GBs. However, the optimal surface geometries and the limitations of the PF-TUNA technique for such studies have not yet been identified, and this provides another motivation to study smooth diamond surfaces with different grain sizes.

2. Methods

In this experiment, PF-TUNA cantilevers were used [Bruker, CA, USA] with a nominal stiffness of 0.4 N m^{-1}, while a tip coating of conductive Pt-Ir gives a typical tip radius in the range of 20 nm. In this study, PF-TUNA was conducted in ambient conditions using a Multimode VIII AFM with Nanoscope V controller housed in two levels of Faraday shielding, while a low force set-point < 1 nN was utilised to maintain scanning in an attractive surface force regime.

Although it is possible to achieve sub-nm roughness values on diamond films using techniques such as chemical-mechanical polishing (CMP) [24], there was the unwanted possibility that these methods may affect the surface chemistry in unknown ways, such as altering the surface termination from H or O to SiO groups (as CMP often uses silicate abrasives), which in turn, may affect the electron emission. To avoid this issue, we chose to investigate two forms of polycrystalline diamond with low surface roughness with grain sizes ranging from nm to tens of μm produced by two methods not involving CMP. In Sample 1, the nucleation layer of a typical MCD film was measured. A single-crystal aluminium nitride (AlN) substrate with an original r.m.s. surface roughness of ~5 nm was seeded using a suspension of 4–10 nm nanodiamond particles (NanoAmando, Japan) in methanol. A ~4 μm-thick,

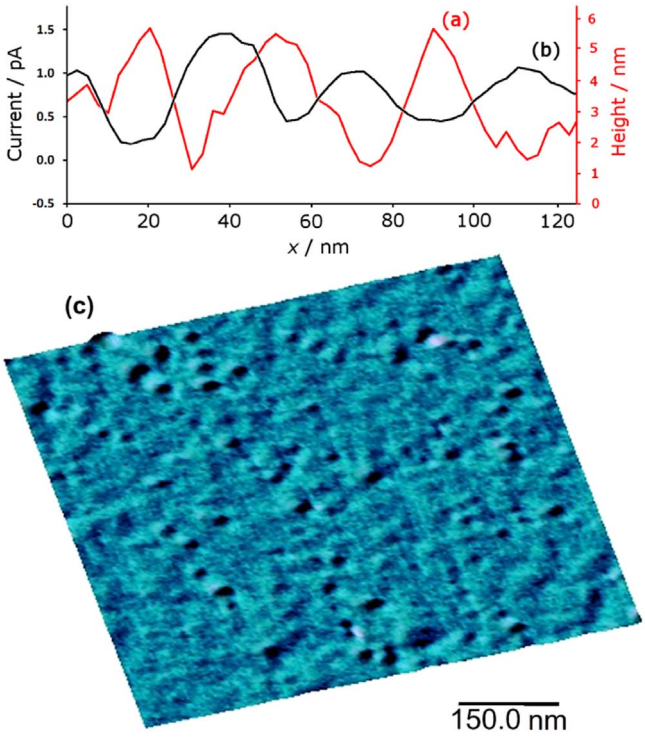

Fig. 2. PF-TUNA measurement (bias 10 mV) of topography and tunnelling current across a representative region of the nucleation side of Sample 1. (a) A line profile of topography across 3 grains and 4 GBs. (b) The corresponding line profile for the measured tunnelling current across the same region. (c) 3D surface showing the nano-smooth topography with the corresponding current overlaid as a blue colour-map (colour scale as in Fig. 1(c)). Because the total current (as estimated by the area under the plot) is larger, the film appears lighter blue overall than the MCD film shown in Fig. 1(c). Also, the emission site density is now so large that on this scale it is difficult to distinguish the non-emitting grains from the emitting grain boundaries. (For interpretation of the references to colour in this figure legend, the reader is referred to the web version of this article.)

undoped (i.e. highly resistive) facetted diamond film was deposited on the seeded substrate under typical MCD growth conditions (5%CH_4/H_2 gas mixture, 1 kW input power, 120 Torr pressure, 800 °C, 2.5 h) in a microwave plasma CVD system [1]. AlN was chosen as the substrate because CVD diamond does not adhere very well to the smooth AlN surface due to the difference in thermal expansion coefficient and the lack of a carbide layer at the interface [25]. Therefore, the diamond film delaminated during the cooling step following CVD to form a freestanding film and allow access to the nucleation surface that had originally been in contact with the AlN. The sample was acid cleaned (50% conc. sulfuric acid, 50% conc. nitric, acid for 3 h) and sonicated in water to remove any surface debris. The acid cleaning had the unwanted side-effect of making the surface oxygen terminated and non-conducting. Therefore, the surface was re-hydrogen-terminated using an H_2 plasma in a microwave CVD reactor for several minutes immediately prior to analysis to make it sufficiently conducting for PF-TUNA analysis.

Sample 2 was a commercial free-standing undoped MCD film (TM100, 10.0 × 10.0 × 0.25 mm, Element Six, UK) that had been mechanically polished to an average roughness (according to the manufacturer's specifications) of < 50 nm. The sample was then acid cleaned and washed, as described above. This treatment was particularly important for Sample 2, as it was necessary to remove the considerable amount of surface debris remaining from the mechanical polishing process. Scanning electron microscopy (SEM) revealed that this treatment removed most of the debris, however, a few isolated nanoparticles remained scattered around the surface. Energy dispersive X-ray analysis confirmed that these particulates were non-metallic and composed only of carbon, while SEM indicated that they were

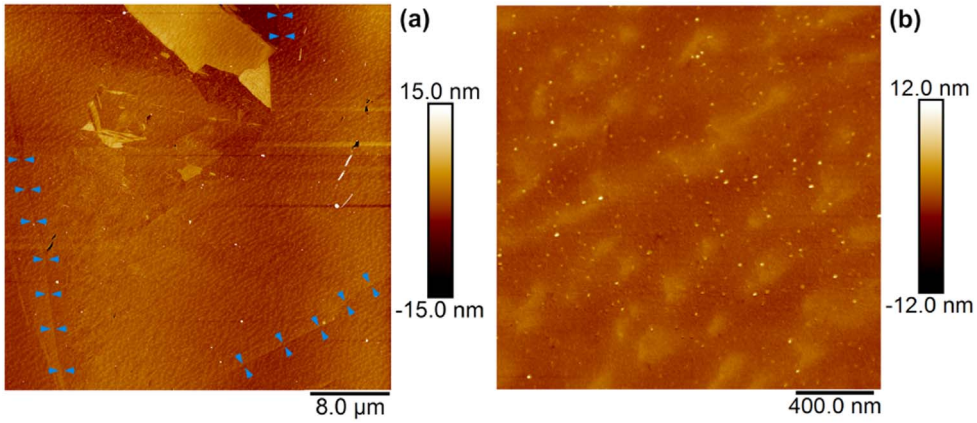

Fig. 3. PF-AFM topographic image of a representative area of Sample 2. (a) A 40 µm × 40 µm region displaying boundaries of large grains, highlighted by arrows. (b) A 2 µm × 2 µm region displaying the nanometre r.m.s roughness of individual facets produced by mechanical polishing. Also evident are debris particles in the range of a few nm, the height range generated by these particles remains consistent over larger scan sizes, as shown by (a).

sufficiently separated not to affect the TUNA measurements. After cleaning, Sample 2 was re-hydrogen-terminated as before.

3. Results and discussion

Fig. 2(a) shows that the surface roughness of the diamond nucleation layer in Sample 1 was ~5 nm, consistent with that of the original AlN substrate, and consists of close-packed diamond features, which have a measured size of 20–40 nm due to convolution with the AFM tip radius. This is expected based upon the size distribution and random nature of the nanoparticle seeding. Despite this surface being smooth on the 10's of nm scale, line profiles across 4 features (Fig. 2(b)) show that measurement of higher emission current directly matches the spacing *between* them. As was previously shown for UNCD films [11], the high density of GBs due to the small grain size means that the percentage of the surface that is emitting is increased. The emission intensity was quantified by measuring the emission current above a threshold set at the r.m.s. current for each sample, to give an estimate for the percentage of the surface area that emits electrons. Using this method we estimate that the small grains present in the nucleation surface of the film result in a percentage surface emission of ~71%; this is greater than that previously reported for UNCD of 49% and significantly larger than the 18% reported for MCD films. This suggests that a diamond surface with the smallest possible grain size, i.e. a high density of grain boundaries, offers the optimum efficiency for an undoped CVD diamond emitter. However, for the demonstration of individual GB emission by PF-TUNA techniques this high density of emission sites can prove challenging because detailed investigation of individual boundaries in this scenario will require a very sharp interaction point between the tip and the sample.

For Sample 2, PF-TUNA measurements revealed that the local film surface was significantly smoother than the quoted specifications, with the surface being comprised of diamond grains with size > 10 µm but with an r.m.s. roughness of 0.67 nm. Indeed, individual large grains and their facets could often be detected only by very small differences in surface angle, as shown in Fig. 3(a) and (b).

Electron emission was recorded at GBs exhibiting this small change in angle between grains (see Fig. 4).

To further demonstrate that topography is not a major factor in emission, Fig. 5 presents an example of a GB from Sample 2 where the grains on either side are the same height and orientation. In this example, increased emission is measured following a linear surface orientation equivalent to that demonstrated in Fig. 4, identifying the presence of a GB. Also, similar to Fig. 4 is the fact that, topographically, the emitting region has no features of greater height than the surface roughness of the surrounding diamond. The lack of discernible surface features corresponding to this GB eliminates the potential for this emission to be due to damage to the surface from the polishing

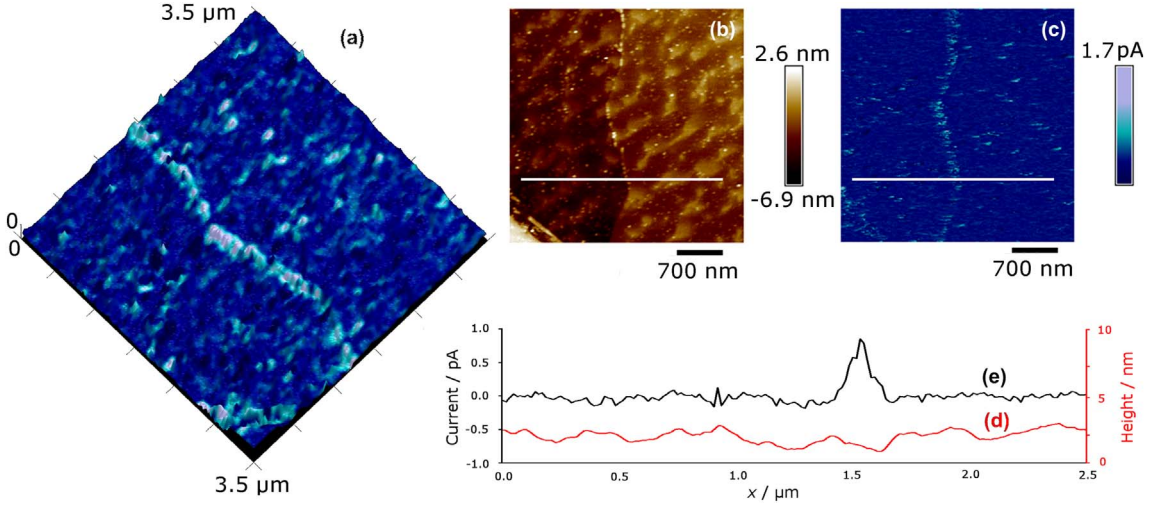

Fig. 4. PF-TUNA measurement (bias 4 V) of topography and tunnelling current across a 3.5 µm × 3.5 µm selected region of Sample 2. (a) 3D surface showing topography with corresponding current overlaid as a blue colour-map (same colour scale as before). (b) Topographical map with slight differences in surface angle identifying the position of the GB, a horizontal line shows the position of the line scan (d). (c) Tunnelling current map of the same area with equivalent line scan shown. (d) A line profile of topography across the GB. (e) The corresponding line profile of measured tunnelling current across the same GB. (For interpretation of the references to colour in this figure legend, the reader is referred to the web version of this article.)

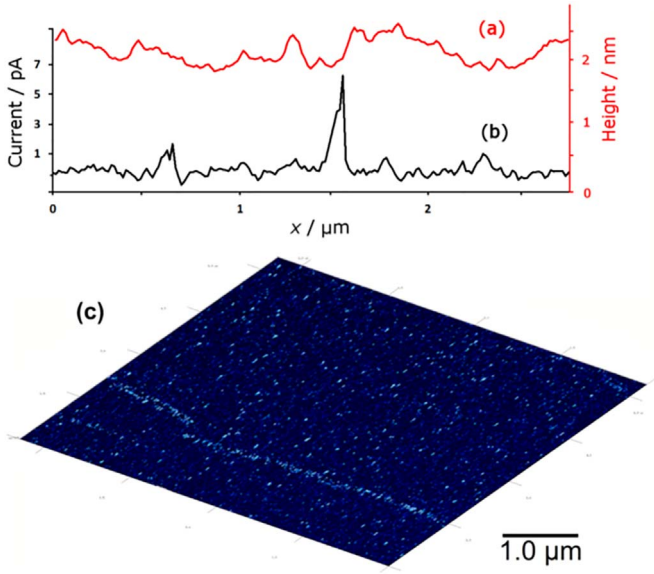

Fig. 5. PF-TUNA measurement (bias 4 V) of topography and tunnelling current across a region of Sample 2 where two smooth, flat crystallites with the same height and orientation meet at a GB. (a) A line profile of topography across the GB, which is situated at $\sim x = 1.5$ µm. (b) The corresponding line profile of measured tunnelling current across the same GB. (c) 3D surface showing topography with corresponding current overlaid as a blue colour-map (same colour scale as before). The surface is uniformly flat, but the position of the GB can be identified clearly by the line of brighter colour indicating increased emission current. (For interpretation of the references to colour in this figure legend, the reader is referred to the web version of this article.)

technique. More importantly it provides a definitive proof that the identification of electron emission sites by PF-TUNA is not due to surface morphology, even down to the nano-scale.

4. Conclusions

We have previously shown that PF-TUNA measurements provide direct evidence that electron emission from poorly conducting polycrystalline CVD diamond samples occurs preferentially from the grain boundaries, and not the grains themselves or from any effect of geometry. Although we had taken precautions to avoid topographic artefacts confounding the data, there was still the possibility that some unknown tip-surface effect with micron-sized features was generating a false conclusion. The results presented here, on smooth diamond surfaces, eliminate any possibility of geometrical artefacts, and so the conclusion about emission arising from grain boundaries is strengthened.

The exact nature of the GBs in diamond films is still unclear, however it is likely that different types of diamond film will have different GB characteristics. For films with large grains, such as the MCD film in Sample 2, the GBs can be almost atomically sharp, and contain many stacking faults and dislocations [26,27,28]. In contrast, the GBs in films with smaller crystallites, such as those found in NCD or in the nucleation surface of MCD films (as in Sample 1) can be a few nm in thickness and often contain significantly more sp^2 carbon impurities [29]. For UNCD films, the GBs are almost the same size as the grains themselves, and contain significant graphitic or other sp^2 carbon phases, as well as H and other impurities [29]. In this paper and previous ones [11,18], we have shown that whatever the nature of the GB, they behave similarly in respect to enhancing electron emission, and they appear to all be consistent with the model for field emission described by Cui et al. [15]. Nevertheless, there may be some subtle differences between the electron emission characteristics from different types of GB, which might be obtained by a future systematic PF-TUNA studies using higher sensitivity equipment. This may provide a method by which to study the nature of GBs in different diamond films in more detail.

One difference between the high-resolution PF-TUNA measurements and macroscopic large-area field emission from diamond is that the latter are often dominated by a small number of hot-spots, from which the majority of the emission originates [10]. Often the emission from these hot-spots is not stable and 'flickers', and with prolonged emission the sites can burn out, to be replaced by new hot-spots which switch on elsewhere on the surface [12]. The PF-TUNA results, in contrast, do not predict such hot-spots, but suggest that, if scaled up, emission would be rather uniform over the whole tested area. One reason for this apparent incongruity probably results from the fact that electrons always take the path of least resistance. When the electric field is applied over a large area, there will always be certain regions on the film surface that have a much lower electrical resistance, as a result of the random conduction pathways (i.e. the GBs in PCD films) from the back contact to the emitting surface having a favourable connective network at those points. The nature of the emission site will probably still be a GB on the surface, however this site will now pass nearly all the emission current, until the localised heating causes it to restructure into a less conducting form, or it permanently burns out. It is unlikely that the PF-TUNA tip would be fortunate enough to scan across one of these hot-spots by chance, and so these measurements will necessarily be representative of the general electron emission properties of the surface rather than those of the hot-spots.

The results suggest that smooth polished diamond films are ideal candidates for more advanced PF-TUNA studies of GBs, including measurements of the surface barrier structure, Fermi level positioning and the electron supply function. However, once the position of the GB was identified, this would probably require extremely high-resolution PF-TUNA to map out the GB on the atomic scale.

Acknowledgements

The authors thank Alex Croot for hydrogenating the diamond samples. PeakForce AFM/TUNA was carried out in the Chemical Imaging Facility, University of Bristol with equipment funded by EPSRC under Grant "*Atoms to Applications*" EP/K035746/1. Raw data and high-resolution images for this paper are available in the online University of Bristol data repository: http://dx.doi.org/10.5523/bris.2xnbyqzab1r3c2digpw0v1o8qd.

References

[1] P.W. May, Diamond thin films: a 21st century material, Philos. Trans. R. Soc. Lond. A 358 (2000) 473–495.
[2] J. van der Weide, Z. Zhang, P.K. Baumann, M.G. Wensell, J. Bernholc, R.J. Nemanich, Negative-electron-affinity effects on the diamond (100) surface, Phys. Rev. B 50 (1994) 5803.
[3] S.V. Baryshev, S. Antipov, J.H. Shao, C.G. Jing, K.J.P. Quintero, J.Q. Qiu, W.M. Liu, W. Gai, A.D. Kanareykin, A.V. Sumant, Planar ultrananocrystalline diamond field emitter in accelerator radio frequency electron injector: performance metrics, Appl. Phys. Lett. 105 (2014) 203505.
[4] K.J.P. Quintero, S. Natipov, A.V. Sumant, C.G. Jing, S.V. Baryshev, High quantum efficiency ultrananocrystalline diamond photocathode for photoinjector applications, Appl. Phys. Lett. 105 (2014) 123103.
[5] F.A.M. Koeck, R.J. Nemanich, Y. Balasubramaniam, K. Haenen, J. Sharp, Enhanced thermionic energy conversion and thermionic emission from doped diamond films through methane exposure, Diam. Relat. Mater. 20 (2011) 1229–1233.
[6] J.S. Lapington, V. Taillandier, B.L. Cann, J. Howorth, J. Milnes, R. Vaz, P.W. May, N.A. Fox, R. Stevens, L. Wang, Investigation of the secondary electron emission characteristics of alternative dynode materials for imaging photomultipliers, J. Instrum. 7 (2012) E04002({Erratum to: J. Instrum. 7 (2012) C03018}).
[7] Y. Zou, P.W. May, S.M.C. Vieira, N.A. Fox, Field emission from diamond-coated multiwalled carbon nanotube 'teepee' structures, J. Appl. Phys. 112 (2012) 044903.
[8] J.L. Davidson, W.P. Kang, K. Subramanian, Y.M. Wong, Forms and behaviour of vacuum emission electronic devices comprising diamond or other carbon cold cathode emitters, Phil. Trans. R. Soc. A 366 (2008) 281.
[9] R.H. Fowler, L. Nordheim, Electron emission in intense electric fields, Proc. R. Soc. London, Ser. A 119 (1928) 173.
[10] O. Chubenko, S.S. Baturin, K.K. Kovi, A.V. Sumant, S.V. Baryshev, Electron Emission Area Depends on Electric Field and Unveils Field Emission Properties in

Nanodiamond Films, (2017) (arXiv:1703.04033v1 [cond-mat.mtrl-sci]).
[11] R.L. Harniman, O.J.L. Fox, W. Janssen, S. Drijkoningen, K. Haenen, P.W. May, Direct observation of electron emission from grain boundaries in CVD diamond by PeakForce-controlled tunnelling atomic force microscopy, Carbon 94 (2015) 386–395.
[12] P.W. May, S. Höhn, M.N.R. Ashfold, W.N. Wang, N.A. Fox, T.J. Davis, J.W. Steeds, Field emission from chemical vapor deposited diamond and diamond-like carbon films: investigations of surface damage and conduction mechanisms, J. Appl. Phys. 84 (1998) 1618–1625.
[13] M.W. Geis, N.N. Efremow, K.E. Krohn, J.C. Twichell, T.M. Lyszczarz, R. Kalish, J.A. Greer, M.D. Tabat, A new surface electron-emission mechanism in diamond cathodes, Nature 393 (1998) 431–435.
[14] D. Pradhan, I.N. Lin, Grain-size-dependent diamond-nondiamond composite films: characterization and field-emission properties, ACS Appl. Mater. Interfaces 1 (2009) 1444–1450.
[15] J.B. Cui, J. Ristein, L. Ley, Low-threshold electron emission from diamond, Phys. Rev. B 60 (1999) 16135.
[16] J. Robertson, Mechanisms of electron field emission from diamond, diamond-like carbon, and nanostructured carbon, J. Vac. Sci. Technol. B 17 (1999) 659–665.
[17] A.C. Ilie, A.C. Ferrari, T. Yagi, S.E. Rodil, J. Robertson, E. Barborini, P. Milani, Role of sp^2 phase in field emission from nanostructured carbons, J. Appl. Phys. 90 (2001) 2024–2032.
[18] V. Chatterjee, R. Harniman, P.W. May, P.K. Barhai, Direct observation of electron emission from the grain boundaries of chemical vapour deposition diamond films by tunneling atomic force microscopy, Appl. Phys. Lett. 104 (2014) 171907.
[19] A.V. Karabutov, V.D. Frolov, S.M. Pimenov, V.I. Konov, Grain boundary field electron emission from CVD diamond films, Diam. Relat. Mater. 8 (1999) 763–767.
[20] K.J. Sankaran, K. Panda, B. Sundaravel, N.H. Tai, I.N. Lin, Enhancing electrical conductivity and electron field emission properties of ultrananocrystalline diamond films by copper ion implantation and annealing, J. Appl. Phys. 115 (2014) 063701.
[21] A.R. Krauss, O. Auciello, M.Q. Ding, D.M. Gruen, Y. Huang, V.V. Zhirnov, E.I. Givargizov, A. Breskin, R. Chechen, E. Shefer, V. Konov, S. Pimenov, A. Karabutov, A. Rakhimov, N. Suetin, Electron field emission for ultra-nanocrystalline diamond films, J. Appl. Phys. 89 (2001) 2958.
[22] O. Chubenko, S.S. Baturin, S.V. Baryshev, Scanning probe microscopy and field emission schemes for studying electron emission from polycrystalline diamond, Appl. Phys. Lett. 109 (2016) 113102.
[23] H. Zanin, P.W. May, M.H.O.M. Hamanaka, E.J. Corat, Field emission from hybrid diamond-like carbon and carbon nanotube composite structures, ACS Appl. Mater. Interfaces 5 (2013) 12238–12243.
[24] E.L.H. Thomas, G.W. Nelson, S. Mandal, J.S. Foord, O.A. Williams, Chemical mechanical polishing of thin film diamond, Carbon 68 (2014) 473–479.
[25] J. Cervenka, D.W.M. Lau, N. Dontschuk, O. Shimoni, L. Silvestri, F. Ladouceur, S.G. Duvall, S. Prawer, Nucleation and chemical vapor deposition growth of polycrystalline diamond on aluminum nitride: role of surface termination and polarity, Cryst. Growth Des. 13 (2013) 3490–3497.
[26] J. Narayan, Dislocations, twins, and grain boundaries in CVD diamond thin films: atomic structure and properties, J. Mater. Res. 5 (1990) 2414–2423.
[27] N. Bozzolo, S. Barrat, I. Dieguez, E. Bauer-Grosse, Spatial distribution of stacking faults and microtwins in isolated crystals and textured diamond films, Diam. Relat. Mater. 5 (1996) 1532–1535.
[28] Y. Zhang, H. Ichinose, M. Nakanose, K. Ito, Y. Ishida, Transmission electron microscopic observation of grain boundaries in CVD diamond thin films, J. Electron Microsc. 45 (1996) 436–441.
[29] O.A. Williams, Nanocrystalline diamond, Diam. Relat. Mater. 20 (2011) 621–640.